

CAAP Quarterly Report 5

12/30/2024

Project Name: "Bio-Inspired Rational Design of Bio-Based Inhibitors for Mitigating Internal Corrosion in Metal Pipelines"

Contract Number: 693JK32350003CAAP

Prime University: University of Miami

Prepared By: Sevil Ozsut and Dr. Ali Ghahremaninezhad; a.ghahremani@miami.edu; 305-284-3465

Reporting Period: 10/01/2024-12/30/2024

Project Activities for Reporting Period:

This report investigates the inhibitive effects of various proteins, bio-based surfactants, and synthesized inhibitors, specifically poly-aspartic acid (PASP) and methionine-functionalized poly-aspartic acid (PASP-M), through electrochemical and weight loss analyses. The efficiency of these inhibitors was evaluated using electrochemical techniques, including open circuit potential (OCP) and electrochemical impedance spectroscopy (EIS), facilitating a comparative assessment of the inhibitory performance of the different test inhibitors. Surface characterization of the A36 steel specimens was also conducted to examine any morphological changes. The study utilized 0.5 M HCl and 3.5% NaCl solutions as corrosive environments to compare the inhibition efficiencies of the inhibitors in two distinct corrosive media. Additionally, the A36 steel specimens were subjected to dynamic flow conditions within a pipeline system, designed to investigate the impact of specimen position within the pipeline and the corresponding inhibition efficiency of the test inhibitors under these conditions.

1. Materials and Methods

1.1. Materials

The amino acids (reagent grade $\geq 98\%$), L-aspartic acid, L-methionine, and proteins were purchased from Sigma-Aldrich and used without further purification. The commercially available surfactants were used as inhibitors. The inhibitors used and their abbreviations are listed in Table 1.

Table 1: List of inhibitors and their abbreviations used in the study

Name	Abbreviation	Name	Abbreviation
------	--------------	------	--------------

Poly-aspartic acid	PASP	Methionine-functionalized poly-aspartic acid	PASP-M
Soy Protein	SP	Imbentin T400	I-T400
Imbentin AG168-S500	I-AG168	Imbentin C91-025	I-C91
Greenbentin LM-010	G-LM010		

A36 steel specimens (McMaster-Carr, US) with the composition of C: 0.19%, Cr: 0.04%, Cu: 0.03%, Mn: 0.76%, Mo: 0.01%, Ni: 0.01%, Si: 0.019%, P: 0.01%, S:0.008%, V: 0.001% and Fe: remainder were used in all the experimental studies. The specimen dimensions used in the weight loss experiment were 20 mm x 10 mm x 2 mm. For the electrochemical tests, the circular-shaped specimens were fixed in an electrode holder made of polytetrafluoroethylene (PTFE) to have 1 cm² as the reacted area. Before experiments, the specimens' surfaces were mechanically polished with silicon carbide (SiC) papers with a grit size of #180, #320, and #600. The specimens were then rinsed with deionized water and acetone, followed by air drying. Before any experiment, the specimens were treated as described and freshly used with no further storage.

The electrolyte solution of 0.5 M HCl was prepared by diluting 37% analytical-grade HCl (Sigma-Aldrich) with deionized water. A 3.5% NaCl solution was also prepared by dissolving 35 g of NaCl in 1 L of deionized water. The inhibitors were dissolved separately in the 0.5 M HCl solution and the 3.5% NaCl solution to achieve concentrations of 0.5 g/L and 1 g/L.

Furthermore, a chemical functionalization method was employed to design a novel PASP and PASP-M through the ring-opening reaction of polysuccinimide (PSI) with methionine, as sulfur-containing compounds are known to exhibit a strong affinity for the steel surfaces in acidic solutions [1]

1.2. Weight Loss Measurements

The weight loss measurements were performed to assess and compare the corrosive behavior of A36 steel specimens exposed to various corrosive environments, which are 0.5M HCl solution and 3.5% NaCl solution. These measurements provide quantitative data on the material degradation due to corrosion, facilitating an understanding of how different environments influence the corrosion rate. By evaluating weight loss over time, it is possible to establish a correlation between environmental factors and the rate of corrosion, offering insights into the performance and durability of A36 steel in diverse conditions. The weight loss was measured as the difference between the weight at a given time and the initial weight of the specimens. A36

steel specimens (20mm x 10mm x 2mm) were immersed in corrosive solutions for 1 day, 3 days and 7 days measurements. After immersion periods, the steel specimens were rinsed with deionized water and acetone, dried in air, and reweighed. Furthermore, the synthesized inhibitors, PASP and PASP-M, were analyzed to evaluate their effectiveness in mitigating corrosion in a 0.5M HCl solution.

Three replicates were used for each test. The average relative mass loss of the A36 steel specimens was determined from three individual measurements. All the measurements were taken at room temperature. The corrosion rate (CR) and inhibition efficiency (IE) were calculated by the following equations:

$$CR (mmy) = \frac{KW}{\rho At} \quad (1)$$

where W is the weight loss (in g), ρ is the density (gcm^{-3}), A is the exposed area of the specimen (cm), and t is the exposure time (h). K is a constant that can be varied to calculate the corrosion rate in various units. For the case of mm/year for CR calculation, K is equal to 8.75×10^4 .

$$IE_{WL}(\%) = \frac{CR_0 - CR_i}{CR_0} \times 100 \quad (2)$$

where CR_0 and CR_i are the corrosion rates of A36 steel in the absence and presence of inhibitors respectively.

1.3. Electrochemical Measurements

Electrochemical experiments including OCP and EIS were conducted in a conventional three-electrode glass cell, using a Gamry Reference 600 and Gamry 1010E potentiostats. A36 steel specimens were used as the working electrode. The saturated calomel electrode (SCE) and platinum sheet electrode were used as a reference electrode and counter electrode, respectively. The details of the experimental setup have been provided in the 2nd quarter report. All the electrochemical experiments were repeated three times to examine the reproducibility of the electrochemical data. The obtained EIS data was interpreted by Gamry Echem Analyst. With the EIS results, corrosion IE was calculated according to Equation 3.

$$IE_{EIS}(\%) = \frac{R_{ct} - R_{ct,0}}{R_{ct}} \times 100 \quad (3)$$

where $R_{ct,0}$ and R_{ct} are the charge transfer resistance without and with inhibitor, respectively.

1.4. Surface Characterization Techniques

1.4.1 Fourier Transform Infrared Spectroscopy (FTIR)

The FTIR analysis was performed using a Perkin Elmer Frontier spectrometer with an ATR accessory, to determine the structure and bond configuration of the inhibitors and the formed film on the A36 steel surface. The FTIR spectra of PASP-M and the resulting complex film formed on the A36 steel specimen were obtained following 24 hours of immersion in a 0.5 M HCl solution containing 0.5 g/L of the inhibitor. This analysis aimed to investigate the interactions between the inhibitor and the steel surface, providing insight into the chemical composition and bonding mechanisms involved in the formation of the protective film. The FTIR spectra of both PASP-M and the complex film were compared to assess the effectiveness of PASP-M in inhibiting corrosion and its ability to form a stable protective layer on the steel surface under acidic conditions. The transmission infrared spectra of the specimens were recorded in the range between 650 cm^{-1} and 4000 cm^{-1} at a resolution of 4 cm^{-1} . The background noise was also collected and removed from both the inhibitor and A36 steel spectra. After obtaining the spectra, baseline correction was applied to the spectra to fix both the sloping shape of the spectra and the offset in absorbance.

1.4.2 UV-Visible Spectroscopy (UV-Vis)

UV-Vis analysis was performed using a Shimadzu UV-2600 spectrophotometer, covering a wavelength range of 200-800 nm. UV-Vis spectra were recorded for 0.5 g/L PASP-M solutions in 0.5 M HCl, both before and after the immersion of A36 steel specimens for 24 hours. The spectral profiles were subsequently compared to determine whether a complex was formed between the PASP-M molecules and Fe^{2+} ions in the solution.

1.4.3 Scanning Electron Microscope (SEM) and Energy Dispersive X-ray Spectroscopy (EDS)

The surface morphology of the A36 steel specimens, both before and after immersion in a 0.5 M HCl solution, was examined using a JEOL JSM 6010PLUS SEM. This analysis was carried out in both the absence and presence of PASP-M. SEM micrographs of the polished, corroded steel surfaces, as well as those treated with PASP-M, were captured at an accelerating voltage of 15 kV and 1000x magnification. The protective film formed as a result of the inhibition process was further analyzed and chemically characterized using EDS system integrated with the JEOL JSM 6010PLUS SEM.

1.5. Pipeline System (Dynamic Condition)

The corrosion mitigation on A36 steel using inhibitors was analyzed within a laboratory-scale pipeline system. A custom-designed model was developed to simulate real-world pipeline conditions and to evaluate the effectiveness of test inhibitors under dynamic flow conditions. The experimental setup is shown in Figure 1. The apparatus comprises a PVC pipe with an internal diameter of 1.278 inches. The A36 steel specimens were machined into dimensions of 20 mm x

10 mm x 1.5 mm. These specimens were strategically positioned on the inner walls of the pipe, corresponding to the top, bottom, left, and right orientations. Each steel specimen was securely attached to the pipe using external magnets, as illustrated in Figure 1. The purpose of this placement was to investigate positional variations in corrosion behavior along the pipeline under consistent flow conditions.



Figure 1: A laboratory-scale pipeline system.

The corrosion medium used in this study was 0.5 M HCl solution, circulated through the pipeline at a flow rate of 3.5 gallons per minute (GPM) using a vacuum pump. A blue container served as the reservoir for the corrosive solution.

For the no inhibitor case (control), the A36 steel specimens were individually weighed to establish their initial mass and attached to the pipeline system. Then, A36 steel specimens were exposed to the circulating 0.5 M HCl solution for 3 days. After the exposure period, the specimens were removed, cleaned, and reweighed to determine weight loss due to corrosion. This initial test provided baseline data on corrosion rates under uninhibited conditions. Additionally, the effects of fluid dynamics on corrosion rates were evaluated based on the position of the steel specimens within the pipeline.

To measure the inhibition effect of the test inhibitor, A36 steel specimens were subjected to a 3-hour coating process using PASP-M. The coated specimens were attached to the pipeline, and the 0.5 M HCl solution was circulated for 3 days under identical conditions. After this period, the specimens were removed and weighed to measure the effect of the inhibitor on corrosion reduction. This comparison allowed for an evaluation of the inhibitor's performance in mitigating corrosion under continuous flow conditions.

The lab-scale experimental pipe model provides a framework for investigating the effects of corrosion inhibitors under controlled conditions. By simulating pipeline environments, this study contributes to the broader understanding of corrosion dynamics and the development of effective strategies for corrosion mitigation in industrial applications. It represents the initial phase of ongoing research aimed at understanding the mechanisms of corrosion inhibition and optimizing inhibitor performance in dynamic environments. Subsequent experiments will investigate the long-term effects of the inhibitor, varying concentrations of the corrosive medium, and different flow rates. The influence of other environmental factors and the development of novel inhibitor formulations will also be explored.

2. Results and Discussion

2.1. Gravimetric Measurements

The corrosion behavior of A36 steel specimens in 0.5 M HCl solution and 3.5% NaCl solution was studied using a weight loss technique and data obtained after 1 day, 3 days, and 7 days of immersion are shown in Table 2. The results indicated that the corrosion rate in the 0.5M HCl solution was significantly higher compared to the 3.5% NaCl solution. This difference can be attributed to the more aggressive acidic nature of the HCl solution, which promotes faster metal dissolution. The experiments were based on weight loss analysis, where the steel specimens were immersed in the respective solutions for a specified period, and the reduction in weight was recorded as an indicator of the corrosion process. These findings highlight the critical role of the corrosive medium in influencing the corrosion behavior of steel, with HCl demonstrating a more severe impact on material degradation than NaCl.

Table 2: The weight loss parameters obtained for A36 steel specimens in 0.5 M HCl solution and 3.5% NaCl solution.

Corrosive Solution	Day 1		Day 3		Day 7	
	CR (mm/year)	IE (%)	CR (mm/year)	IE (%)	CR (mm/year)	IE (%)
0.5 M HCl	5.11	-	4.65	-	4.69	-
3.5% NaCl	0.12	-	0.14	-	0.10	-

The effect of the addition of PASP and PASP-M at various concentrations (0.01 g/L to 0.5 g/L) on the corrosion of A36 steel specimen was studied by the weight loss method for 1 day, 3 days, and 7 days immersion periods in 0.5 M HCl solution. The obtained parameters are presented in Table 3. It was observed that the CR of A36 steel specimens was reduced in the presence of both PASP and PASP-M as compared to the absence of the inhibitors in 0.5 M HCl solution and depends upon the used inhibitor concentration. It can be stated that the CR of A36 steel is

reduced in the presence of inhibitors as compared to the absence of the inhibitor in the solutions. Therefore, the IE increases with the presence of the inhibitor in the corrosive solution. The increased IE indicates that the inhibitor molecules are adsorbed on the A36 steel surface, so, it leads to greater surface coverage and hence the formation of a protective film [2]. This phenomenon was observed for all immersion times of the analysis of PASP and PASP-M. The maximum IE of PASP and PASP-M was found to be 61.7 % and 85.3 %, respectively in 0.5 M HCl at a concentration of 0.5 g/L at 7 days.

Table 3: Weight loss parameters for A36 steel in 0.5M HCl solution without and with various concentrations of PASP-M and PASP for 1 day, 3 days and 7 days immersion periods.

Inhibitor	Concentration (g/L)	Day 1		Day 3		Day 7	
		CR (mmy)	IE (%)	CR (mmy)	IE (%)	CR (mmy)	IE (%)
0.5 M HCl	-	5.11	-	4.65	-	4.69	-
PASP-M	0.01	2.79	45.4	2.39	48.5	2.43	48.2
	0.05	2.18	57.3	1.65	64.4	1.46	68.8
	0.1	1.76	65.5	1.30	72.0	1.11	76.4
	0.5	1.43	69.2	0.88	81.0	0.69	85.3
PASP	0.01	2.94	42.5	2.57	44.7	2.62	44.1
	0.05	2.85	44.2	2.12	54.4	2.13	54.7
	0.1	2.52	50.8	2.07	55.5	2.10	55.2
	0.5	2.32	54.6	1.89	59.3	1.80	61.7

The inhibition is caused by forming a monomolecular film-adsorbed surface, which blocks the direct contact between metal and a corrosive environment [3]. This film is formed by chemical or physical adsorption of the inhibitors onto the metal surface with the formation of a coordinate covalent bond or electrostatic interaction respectively. At the same concentration of the inhibitors, the maximum IE of 85.3 % was observed in the presence of PASP-M in 0.5M HCl solution. This could be attributed to the polymers' ability to form a dense film on the A36 steel specimen, which mainly comes from the functional group in their molecular structure [4]. Since organic inhibitors work by attaching themselves to the metal surface, their effectiveness is heavily influenced by their ability to form a complex film on the metal surface [5]. The presence of heteroatoms containing N, O, P, and/or S, as well as aromatic rings, and the π electrons in their bond structure are fundamental characteristics of the organic inhibitors [6].

2.2. Electrochemical Measurements

The inhibition performance of the inhibitors on A36 steel corrosion in 0.5 M HCl solution and in 3.5% NaCl was investigated using the EIS measurements. The EIS results were analyzed using an

electrical equivalent circuit as shown in Figure 2. In this circuit, R_s represents the solution resistance between the reference and the working electrodes, R_{ct} represents the charge-transfer resistance at the metal-electrolyte interface, and C_{dl} represents the double-layer capacitance. The constant phase element (CPE) instead of C_{dl} was used in the calculation. The use of CPE allows to compensate for the deviation from the ideal dielectric behavior caused by the inhomogeneous nature of the electrode surface [7]. The impedance function of CPE can be described by Equation 4.

$$Z_{CPE} = Y_0^{-1} (j\omega)^{-n} \quad (4)$$

where Y_0 is the magnitude of CPE, j is an imaginary number ($j^2 = -1$), ω is the angular frequency ($=2\pi f$) and exponent n is the deviation parameter and takes on values between -1 to 1. Based on the values of n , CPE can represent: inductance ($n = -1$), resistance ($n = 0$), Warburg impedance ($n = 0.5$), and capacitance ($n = 1$) [15]. The C_{dl} can be obtained by Equation 5.

$$C_{dl} = Y_0 (\omega_{max})^{n-1} = Y_0 (2\pi f_{Z_{im-max}})^{n-1} \quad (5)$$

where ω_{max} is the frequency at which the imaginary impedance has the highest value.

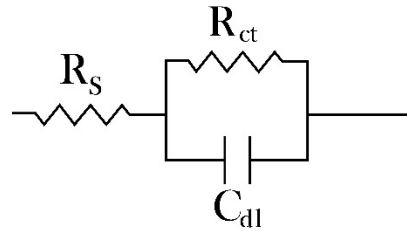


Figure 2: Electrochemical equivalent circuit used to fit the impedance spectra.

In Table 4 and Table 5, the electrochemical parameters, R_s and R_{ct} , obtained from the EIS tests, are presented. Table 4 presents the results of the 0.5 M HCl solution case, and Table 5 presents the results of the 3.5% NaCl solution case. The results are for the concentration of 1 g/L for all inhibitors.

Table 4: EIS parameters for A36 steel in 0.5 M HCl and the presence of the investigated inhibitors.

Inhibitors	R_s ($\Omega \text{ cm}^2$)	R_{ct} ($\Omega \text{ cm}^2$)	IE (%)
0.5 M HCl	3.9	65.5	-
SP	3.8	258.5	74.1
I-C91	3.9	203.8	67.0

I-T400	3.6	170.3	61.3
G-LM010	4.0	169.2	60.0
I-AG168	4.0	148.8	55.4

Table 5: EIS parameters for A36 steel in 3.5% NaCl and the presence of the investigated inhibitors.

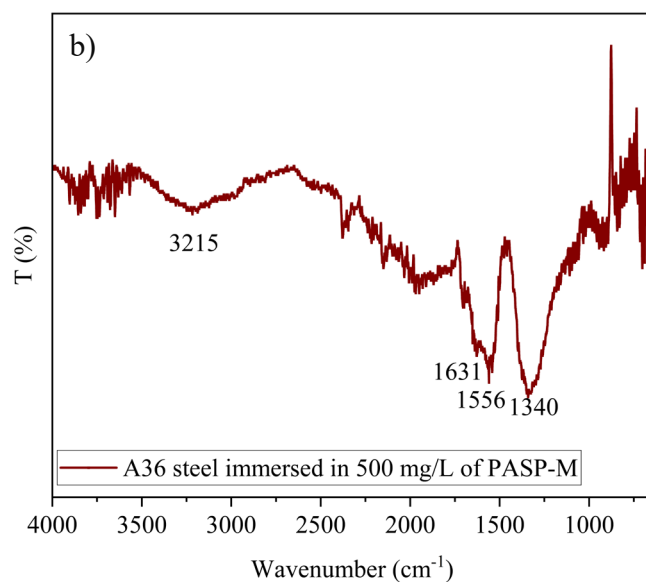
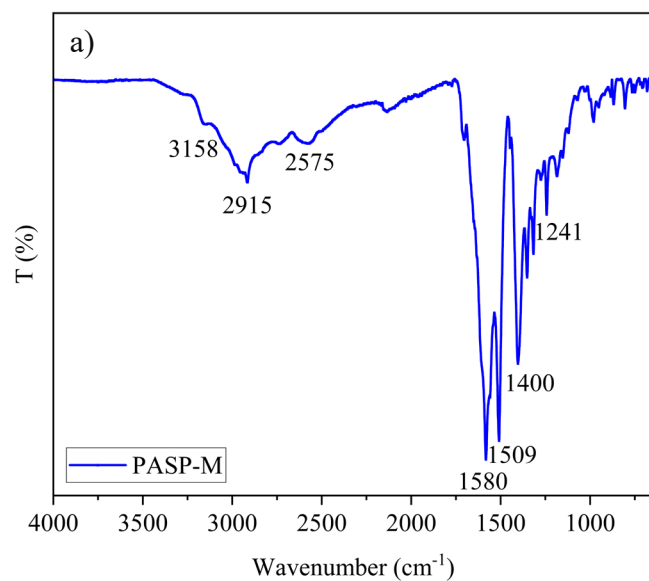
Inhibitors	R_s (Ω cm ²)	R_{ct} (Ω cm ²)	IE (%)
3.5% NaCl	13.2	826.7	-
SP	12.5	1185.2	24.9
I-T400	12.8	1100.8	24.0
G-LM010	13.2	934.8	11.5
I-C91	12.0	907.4	8.9
I-AG168	11.8	736.0	-12.3

From Table 4 and Table 5, it is observed that there was a significant enhancement in the change of R_{ct} with the inhibitors, except I-AG168 in 3.5% NaCl solution, in the corrosive solutions. An increase in R_{ct} manifests the formation of a protective layer on the metal surface, which provides higher resistance toward the charge transfer reactions occurring at the metal-electrolyte interface [8]. The obtained R_{ct} allowed to calculate their efficiency in terms of inhibition of corrosion. The efficiency of the test inhibitors showed greater performance in 0.5 M HCl solution compared to 3.5% NaCl solution.

2.3. Surface Characterization Techniques

2.3.1 FTIR

The A36 steel surface was analyzed using FTIR to observe the formation of the protective layer in the case of 0.5 M HCl solution with the presence of PASP-M. The spectra for the PASP-M, and the surface of A36 steel immersed in 0.5 M HCl with 0.5 g/L PASP-M are presented in Figure 3.



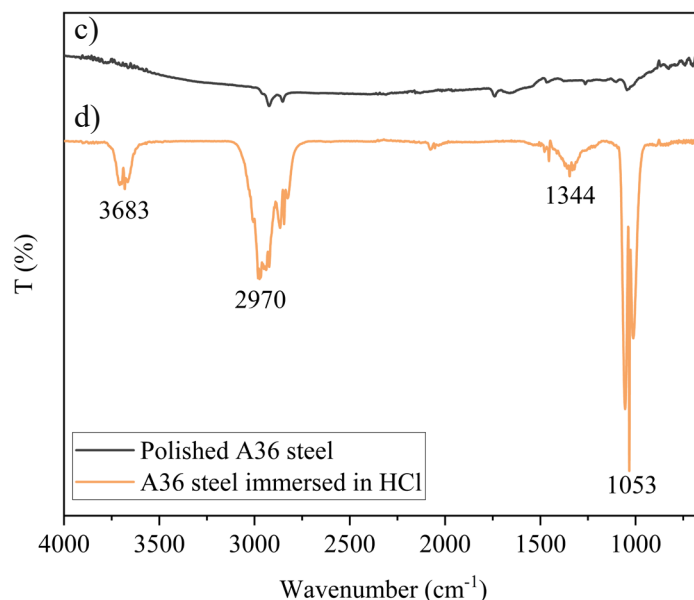


Figure 3: FTIR spectra of a) PASP-M, b) A36 steel immersed in 0.5 M HCl solution with 0.5 g/L PASP-M for 24 hours, c) polished A36 steel, and d) A36 steel immersed in 0.5 M HCl solution without PASP-M for 24 hours.

According to the FTIR spectra of PASP-M, the strong peaks are observed in the 1500-1580 cm⁻¹ range, which are attributed to C=O stretching [9], and a peak at 1400 cm⁻¹ corresponding to the bending vibration of the N-H bond and C-N stretching in the -CONH group [10]. Moreover, the peak at 3158 cm⁻¹ is observed, which is assigned to N-H stretching [11]. Compared with the FTIR spectrum of the A36 steel specimen immersed in 0.5 M HCl solution in the presence of 0.5 g/L PASP-M (Figure 3b), a shift is observed for -NH stretching from 3158 cm⁻¹ to 3215 cm⁻¹. This indicates that the adsorption of PASP-M molecules on the A36 steel surface could take place from the N atom in the PASP-M molecules. Moreover, the C=O stretching peak was shifted to 1631 cm⁻¹ and 1556 cm⁻¹, which suggests a bonding interaction between the carboxyl group of PASP-M molecules and the A36 steel surface. All these reveal the adsorption and interaction of the heteroatoms in PASP-M with the A36 steel specimen surface [12]. It is also observed that the peaks, such as at 2970 cm⁻¹ and 1053 cm⁻¹, for the spectrum of the A36 steel surface immersed in only 0.5 M HCl disappeared when the specimen was immersed in PASP-M containing acidic solution (Figure 3b). Therefore, the presence of PASP-M in corrosive solution provides inhibition for the A36 steel by adsorption onto the surface.

2.3.2 UV-Vis

The UV-Vis spectra were obtained for the solution that contains 0.5 g/L PASP-M in 0.5 M HCl before and after the immersion of the A36 steel specimen for 24 hours. As Figure 4 presents, the obtained absorption spectrum in the UV-Vis region shifted to a higher absorbance value and absorbance band after immersion of A36 steel specimen. This implies that there might be an

interaction between Fe^{2+} and the inhibitor molecules in the solution [13]. Moreover, a displacement in the absorption peaks indicates the interaction between the test inhibitor molecules and Fe^{2+} ions in the solution. Therefore, these results could potentially show the formation of a complex between the Fe^{2+} ions and the PASP-M molecules in 0.5 M HCl solution [14,15].

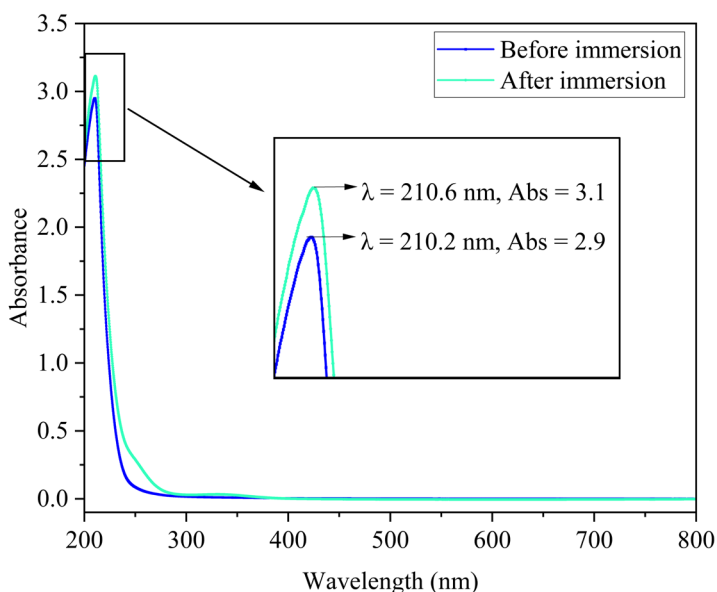


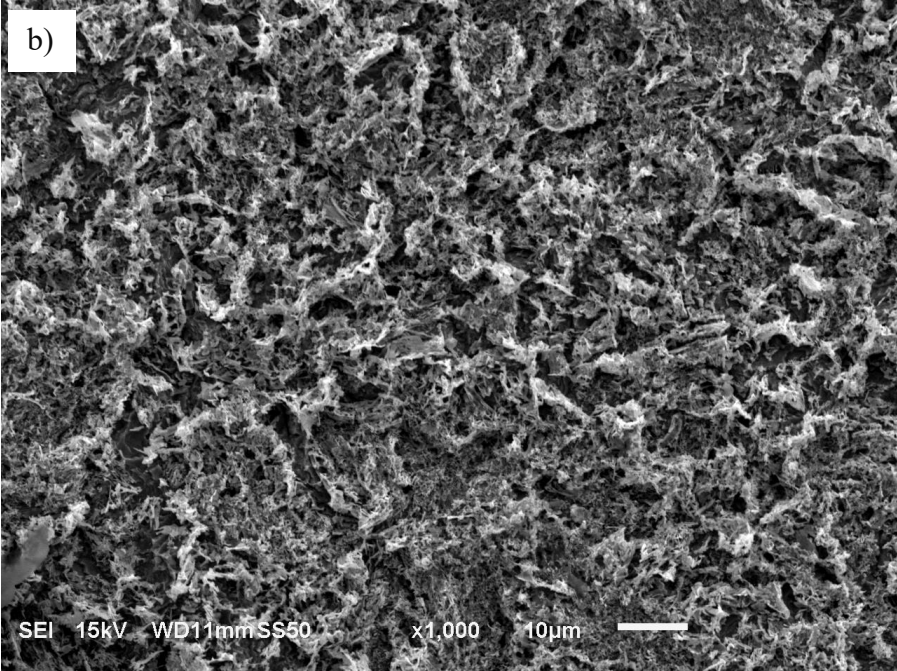
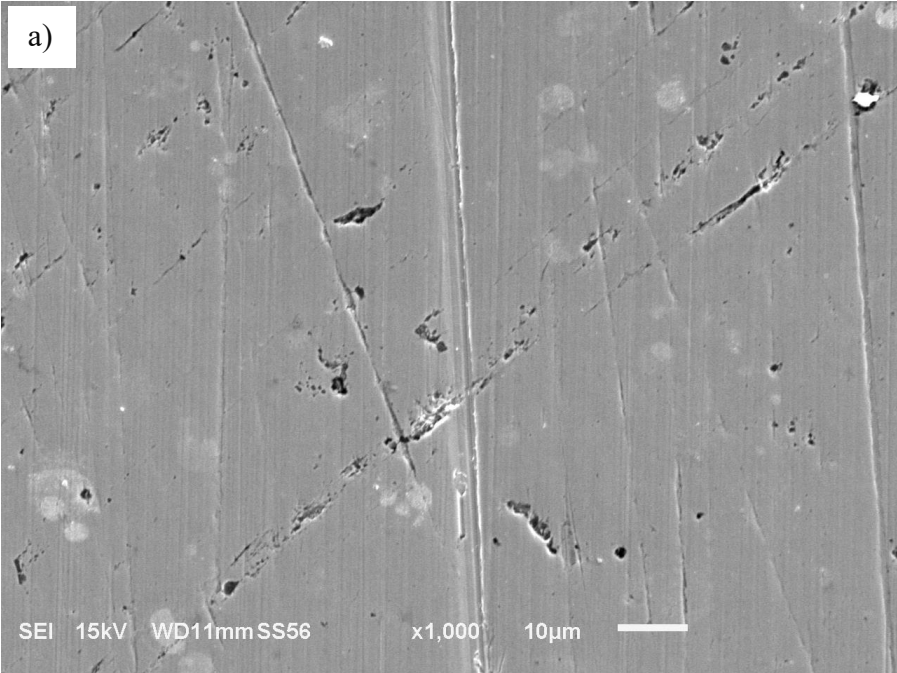
Figure 4: UV-vis spectra of the solutions with 0.5 g/L PASP-M in 0.5 M HCl recorded before and after immersion of A36 steel specimen.

This observed data is explained by having some electronic transitions between the metal surface and the inhibitor molecules, thus, the formation of a film complex on the surface of the A36 steel. The electronic transition can be classified as $n \rightarrow \pi$ or $n \rightarrow \pi^*$ [16]. Having an adsorbed protective film, which was formed by the interaction between the inhibitor molecules and A36 steel surface, can reduce the acid attack on the metal surface. Therefore, corrosion on the surface can be reduced.

2.3.3 SEM-EDS

SEM-EDS provides detailed images of surface morphology and allows for the analysis of the elemental composition of A36 steel. Surface scans of the polished A36 steel specimens, and the specimens after 24 hours of immersion in a 0.5 M HCl solution, both in the absence and presence of 0.5 g/L PASP-M, are presented in Figure 5. Figure 5a shows that the surface of the A36 steel is free from pits and cracks, with only minor scratches present due to the polishing process. On the other hand, the SEM image of the A36 steel specimen immersed in 0.5 M HCl (Figure 5b), shows significant corrosion, with pits and cracks on the surface, indicating extensive damage [12]. However, in the presence of PASP-M, Figure 5c, the surface of the A36 steel appears to be more evenly distributed and compact, compared to the specimen immersed in HCl without the

inhibitor. This suggests that the surface of the A36 steel specimen became appreciably smooth owing to the formation of a protective film by PASP-M over the surface of the steel specimen [17].



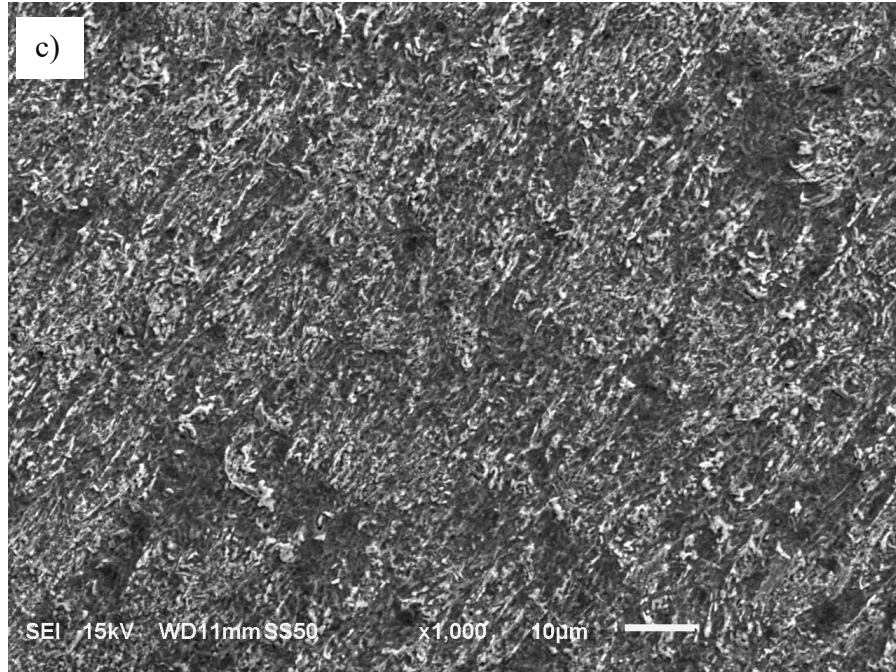


Figure 5: SEM images of a) polished A36 steel specimen, and specimens immersed in 0.5 M HCl for 24 hours b) without PASP-M, (c) with 0.5 g/L PASP-M

Moreover, EDS analysis focuses on the investigation of the adsorption film formed on the surface of the A36 steel specimen. The chemical composition data obtained from the EDS analysis for all specimens were analyzed concerning the characteristic peaks of A36 steel and presented in Table 6. It is observed that the A36 steel surface inhibited with PASP-M shows a higher content of Fe atoms compared to the specimen immersed in 0.5 M HCl solution without PASP-M. Specifically, the mass percentages of Fe atoms are 97.32% for the polished A36 steel surface, 91.35% for the surface immersed in 0.5 M HCl solution without PASP-M, and 94.08% for the surface immersed in 0.5 M HCl solution with 0.5 g/L of PASP-M. These findings indicate that PASP-M molecules absorb onto the A36 steel surface, forming a protective layer that isolates the surface from the corrosive environment [18].

Table 6: Chemical compositions obtained from EDS analysis of polished A36 steel specimen, and specimens immersed in 0.5 M HCl for 24 hours without and with 0.5 g/L PASP-M

Element	Polished A36 steel		Immersed in 0.5M HCl without PASP-M		Immersed in 0.5M HCl with 500 mg/L PASP-M	
	Mass (%)	Atom (%)	Mass (%)	Atom (%)	Mass (%)	Atom (%)
Fe	97.32	89.22	91.35	72.20	94.08	78.11
C	1.67	9.83	7.23	26.56	5.10	19.70

Mn	1.01	0.95	1.27	1.02	0.82	2.19
----	------	------	------	------	------	------

3. Conclusions

The effect of inhibitors, including synthesized PASP and PASP-M, some proteins and surfactants on A36 steel in corrosive solutions (0.5 M HCl solution and 3.5% NaCl solution) were investigated using electrochemical measurements, weight loss analysis and surface characterization methods. The film formation on A36 steel surface and bond formation between inhibitor molecules and steel surface were studied using FTIR and UV-Vis. The surface morphology and chemical composition characteristics were analyzed by performing SEM-EDS. The obtained results showed that the use of inhibitors showed exceptional inhibition efficiency for A36 steel in a corrosive solution. The mechanism for the inhibition could be explained by the adsorption of the inhibitor molecules on the metal surface by their functional groups. The adsorbed molecules of inhibitors formed a complex film on the metal and effectively blocked the steel surface from being attacked by the corrosive media.

Project Financial Activities Incurred during the Reporting Period:

One Graduate Research Assistant (GRA) at the University of Miami.

Materials and Supplies

Advanced Materials Characterization User Fee

Project Activities with Cost Share Partners:

N/A

Project Activities with External Partners:

Collaboration with industry partners has been initiated to investigate the practical implementation of bio-based corrosion inhibitors. This partnership seeks to incorporate industry perspectives into experimental design, ensuring the research addresses real-world challenges and applications. By engaging with industry stakeholders, the methodologies can be refined, and the relevance of the findings to practical scenarios will be strengthened, ultimately promoting the successful adoption of these innovative corrosion prevention solutions.

Potential Project Risks:

N/A

Future Project Work:

Future studies will focus on evaluating multiple types of corrosion inhibitors, including proteins, synthesized molecules, and commercially available formulations. These inhibitors will be tested under varying flow rates and metal specimen positions within the pipeline to analyze the interplay between inhibitor type, flow dynamics, and corrosion mitigation efficiency. The adsorption behavior of the inhibitors will be systematically investigated in both HCl and NaCl solutions, providing comprehensive insights into their performance across different chemical environments and pH conditions.

Particular attention will be given to understanding the impact of molecular weight and chemical structure on the adsorption efficiency and corrosion inhibition performance of the inhibitors. Such findings will contribute to the development of tailored inhibitors optimized for specific industrial applications, enhancing corrosion mitigation strategies in pipeline systems.

Potential Impacts to Pipeline Safety:

The outcomes of this project could significantly transform the creation of environmentally friendly inhibitors and techniques for addressing internal corrosion in pipeline systems.

4. References

- [1] C. Chai, Y. Xu, D. Li, X. Zhao, Y. Xu, L. Zhang, Y. Wu, Cysteamine modified polyaspartic acid as a new class of green corrosion inhibitor for mild steel in sulfuric acid medium: Synthesis, electrochemical, surface study and theoretical calculation, *Prog Org Coat* 129 (2019) 159–170. <https://doi.org/10.1016/j.porgcoat.2018.12.028>.
- [2] M. Mobin, S. Zehra, M. Parveen, L-Cysteine as corrosion inhibitor for mild steel in 1 M HCl and synergistic effect of anionic, cationic and non-ionic surfactants, *J Mol Liq* 216 (2016) 598–607. <https://doi.org/10.1016/j.molliq.2016.01.087>.
- [3] E.E. Oguzie, Y. Li, F.H. Wang, Effect of surface nanocrystallization on corrosion and corrosion inhibition of low carbon steel: Synergistic effect of methionine and iodide ion, *Electrochim Acta* 52 (2007) 6988–6996. <https://doi.org/10.1016/j.electacta.2007.05.023>.
- [4] S. Paramasivam, K. Kulanthai, G. Sadhasivam, R. Subramani, Corrosion Inhibition of Mild Steel in Hydrochloric Acid using 4-(pyridin-2-yl)-N-p-tolylpiperazine-1-carboxamide, *Int J Electrochem Sci* 11 (2016) 3393–3414. [https://doi.org/10.1016/S1452-3981\(23\)17408-6](https://doi.org/10.1016/S1452-3981(23)17408-6).
- [5] S.K. Shukla, M.A. Quraishi, Cefotaxime sodium: A new and efficient corrosion inhibitor for mild steel in hydrochloric acid solution, *Corros Sci* 51 (2009) 1007–1011. <https://doi.org/10.1016/j.corsci.2009.02.024>.
- [6] N.O. Eddy, Experimental and theoretical studies on some amino acids and their potential activity as inhibitors for the corrosion of mild steel, part 2, *J Adv Res* 2 (2011) 35–47. <https://doi.org/10.1016/j.jare.2010.08.005>.
- [7] L. Guo, Y. Luo, Y. Huang, W. Yang, X. Zheng, Y. Lin, R. Marzouki, Imidazolidiny Urea as a Potential Corrosion Inhibitor for Mild Steel in HCl Medium: Experimental and Density-Functional Based Tight-Binding Methods, *Int J Electrochem Sci* 17 (2022). <https://doi.org/10.20964/2022.07.34>.
- [8] S. Satpati, S.K. Saha, A. Suhasaria, P. Banerjee, D. Sukul, Adsorption and anti-corrosion characteristics of vanillin Schiff bases on mild steel in 1 M HCl: Experimental and theoretical study, *RSC Adv* 10 (2020) 9258–9273. <https://doi.org/10.1039/c9ra07982c>.
- [9] A. Pal, S. Dey, D. Sukul, Effect of temperature on adsorption and corrosion inhibition characteristics of gelatin on mild steel in hydrochloric acid medium, *Research on Chemical Intermediates* 42 (2016) 4531–4549. <https://doi.org/10.1007/s11164-015-2295-8>.
- [10] P.M. Nuzaiaba, S. Gupta, S. Gupta, S.B. Jadhao, Synthesis of L-methionine-loaded chitosan nanoparticles for controlled release and their in vitro and in vivo evaluation, *Sci Rep* 13 (2023). <https://doi.org/10.1038/s41598-023-34448-6>.
- [11] P. Singh, K. Bhara, G. Singh, Adsorption and kinetic studies of L-leucine as an inhibitor on mild steel in acidic media, *Appl Surf Sci* 254 (2008) 5927–5935. <https://doi.org/10.1016/j.apsusc.2008.03.154>.

- [12] A.-R.I. Mohammed, M.M. Solomon, K. Haruna, S.A. Umoren, T.A. Saleh, Evaluation of the corrosion inhibition efficacy of *Cola acuminata* extract for low carbon steel in simulated acid pickling environment, (n.d.). <https://doi.org/10.1007/s11356-020-09636-w>/Published.
- [13] M. Finšgar, J. Jackson, Application of corrosion inhibitors for steels in acidic media for the oil and gas industry: A review, *Corros Sci* 86 (2014) 17–41. <https://doi.org/10.1016/j.corsci.2014.04.044>.
- [14] M. El Faydy, B. Lakhrissi, A. Guenbour, S. Kaya, F. Bentiss, I. Warad, A. Zarrouk, In situ synthesis, electrochemical, surface morphological, UV–visible, DFT and Monte Carlo simulations of novel 5-substituted-8-hydroxyquinoline for corrosion protection of carbon steel in a hydrochloric acid solution, *J Mol Liq* 280 (2019) 341–359. <https://doi.org/10.1016/j.molliq.2019.01.105>.
- [15] M. Rbaa, F. Benhiba, A.S. Abousalem, M. Galai, Z. Rouifi, H. Oudda, B. Lakhrissi, I. Warad, A. Zarrouk, Sample synthesis, characterization, experimental and theoretical study of the inhibitory power of new 8-hydroxyquinoline derivatives for mild steel in 1.0 M HCl, *J Mol Struct* 1213 (2020) 128155. <https://doi.org/10.1016/j.molstruc.2020.128155>.
- [16] K. Haruna, I.B. Obot, N.K. Ankah, A.A. Sorour, T.A. Saleh, Gelatin: A green corrosion inhibitor for carbon steel in oil well acidizing environment, *J Mol Liq* 264 (2018) 515–525. <https://doi.org/10.1016/j.molliq.2018.05.058>.
- [17] C. Verma, M.A. Quraishi, K. Kluza, M. Makowska-Janusik, L.O. Olasunkanmi, E.E. Ebenso, Corrosion inhibition of mild steel in 1M HCl by D-glucose derivatives of dihydropyrido [2,3-d:6,5-d'] dipyrimidine-2, 4, 6, 8(1H,3H, 5H,7H)-tetraone, *Sci Rep* 7 (2017). <https://doi.org/10.1038/srep44432>.
- [18] J. Chen, C. Wang, J. Han, B. Hu, C. Wang, Y. Zhong, H. Xu, Corrosion inhibition performance of threonine-modified polyaspartic acid for carbon steel in simulated cooling water, *J Appl Polym Sci* 136 (2019). <https://doi.org/10.1002/app.47242>.